NUMERICAL MODELING AND DESIGN OPTIMIZATION OF A MICRO-CAES SYSTEM

Dario Tumminello[1, *], Tommaso Bacci[1], Bruno Facchini[1]

[1]University of Florence, Department of Industrial Engineering (DIEF), Florence, Italy

*Corresponding Author: dario.tumminello@unifi.it

ABSTRACT

With the increasing demand for electrical energy storage to balance intermittent renewable energy generation, there is a growing interest in efficient and cost-effective storage technologies. Compressed Air Energy Storage (CAES) has emerged as a promising solution due to its long lifetime, low environmental impact and mature technology base. This paper presents the modelling and the optimization of a micro-scale Adiabatic CAES system. Accurately modelling the time-variant behaviour and off-design performance of various components is necessary to estimate the system's performance properly and, consequently, to optimize the design. A model of a micro-CAES was developed using the open-source, object-oriented, software OpenModelica. The storage system is coupled with a PV energy source and an energy user. The model simulates plant behaviour over a year to properly account for the seasonal variations. The model is employed to study the influence of the size of key components on system performance in order to enhance its efficiency through optimized component sizing. The optimization is performed using an external algorithm that guides and steers the optimization process. Six main parameters are selected as design variables such as compressor and expander size, volume and maximum bared pressure of the air storage, TES size, and photovoltaic installed power while round-trip efficiency and energy coverage are selected as a metric for optimization. The sensitivity analysis has shown that the mass of oil exhibits the least influence on system performance among the parameters examined, suggesting its exclusion from the optimization procedure. Through optimization, parameters enabling the achievement of maximal values for each variable have been identified. Additionally, it is shown the utility of the surrogate model developed during optimization for expedited evaluation of system performance throughout the design spectrum.

1 INTRODUCTION

In the last decades the production of electricity from renewable sources has increased constantly leading to a growing need to develop electrical energy storage (EES) technologies (Mohler and Sowder, 2017). Furthermore, there is a growing interest for the development of new small-scale energy storage solutions to shift from centralized to distributed electricity generation, and to ensure energy needs of remote rural areas. Currently, lithium-Ion batteries dominate the field of small and medium size energy storage, but numerous other technologies exist at varying stages of development (T.-T. Nguyen et al., 2017). In this scenario, there is a renewed focus on Compressed Air Energy Storage (CAES). This technology involves compressing air during periods of low electric energy demand, storing it using various types of reservoir volumes, such as salt caverns or pressure vessels, and later releasing it to drive an expander during periods of high energy demand (Garvey and Pimm, 2016). In broad terms CAES systems typically include:

https://doi.org/10.52202/077185-0003

a set of compressor and expander machines, chosen from various categories based on the plant's size (He, 2018); an air reservoir, and, for the so-called Adiabatic-CAES, a Thermal Energy Storage (TES) system, responsible for storing thermal energy generated during the compression phase, to be released during the expansion one (Zhou et al., 2019). CAES systems were traditionally developed for utility-scale application (King et al., 2021) but it is a promising storage technology also at small-scale as it presents a series of benefits if compared with batteries, such as longer lifetime, a far lower environmental impact, a storing capacity that is not subject to degradation and the fact that CAES components are based on mature technology (Dehghani-Sanij et al., 2019; Mucci et al., 2021). Based on this consideration CAES can be considered a competitive alternative to batteries, notwithstanding a lower overall efficiency. Due to its configuration (i.e. storing pressure progressively changing with time) and with the aim of integrating them with renewable sources, small-scale CAES (SS-CAES) must work under transient and off-design conditions (Guo et al., 2019). Nevertheless, as reported by Bazdar et al. (2022), most of the studies presented in literature investigated the CAES performance under design conditions or steady-state mode (Cheayb et al., 2022 Karapekmez et al., 2020). It is also common practice to characterize the system behaviour based on a full charging phase (i.e. from empty reservoir to the point of maximum allowable pressure) and a consequent full discharge. As the actual performance are highly dependent on the actual operation dictated by energy availability/request alternation, the development of time dependent CAES models, is necessary to study the system behaviour over time. Moreover, due the presence of various sub-systems, it is crucial to correctly optimize the system by properly sizing the various components, to avoid CAES under/over-sizing and reduced system's profitability (Heidari et al., 2021).Various design approaches have been proposed to find the optimal size for CAES; some of them are based on analytical procedure (Jannelli et al., 2014) while others are based on the use of optimization algorithms, mainly genetic ones (Congedo et al., 2022; Yao et al., 2016). It is worth to notice that few of proposed approaches try to handle with the dimension of all the components at the same time, as an increased number of parameters significantly affects the capabilities and required time of this approaches. The present work tries to deal with this aspect, showing a system modelling and optimizing procedure that is structured in three main stages. In the first one, a sensitivity analysis is carried out, in order to isolate the main parameters affecting the overall performance of the system, allowing to neglect the others in the following treatment; in the second stage, an optimization procedure is executed based on the Efficient Global Optimization method. This method relies on the use of a Kriging surrogate model to facilitate the optimization process. In the last stage the developed surrogate model is used to investigate the behaviour of the system with a much increased speed, so to deepen the analysis of the system performance and identify optimum configurations when additional constraints are imposed. The application of the paper stays in the description of a methodology that combines different mathematical approaches, to reach a reliable and time-efficient description of the investigated CAES system. The paper is structured as follows: initially, the thermodynamic model is briefly described. Subsequently, the coupling between the thermodynamic solver and the algorithm used for sensitivity analysis and optimization is explained, specifying the mathematical solutions adopted in this phase. Finally, the obtained results are reported.

2 SYSTEM DESCRIPTION

The considered system is an adiabatic micro-CAES; a schematic representation of the plant is shown in 1 It is mainly composed of a three-stages reciprocating compressor, a thermal energy storage system (TES), a series of high-pressure vessels, a lamination valve, and a series of three scroll expanders. The compression phase is intercooled through three heat exchangers that release heat to the oil contained in a reservoir that stores the thermal energy and supplies it back to the air during the discharge phase, and heat sinks that dissipate heat to the ambient. The air is stored in isochoric vessels, causing the compressor outlet pressure to vary based on vessels pressure, while the lamination valve ensures that the pressure at the inlet of the first expander is not higher than a certain allowable value, set at 45 bar. The compressor is driven by an electric motor with variable speed, powered by a series of photovoltaic panels, while the

https://doi.org/10.52202/077185-0003

expanders drive an electric generator that provides power to the users. Further details about the load profile are provided in subsequent sections. The system layout is analogue to the one proposed in a previous work of the authors (Tumminello et al., 2023), where the simplicity of the plan configuration and the use of standard components were a constraint of the work. No innovation is here proposed for the plant layout since the aim of this article is to explore the possibility to build an optimization procedure rather than to propose a novel system configuration.

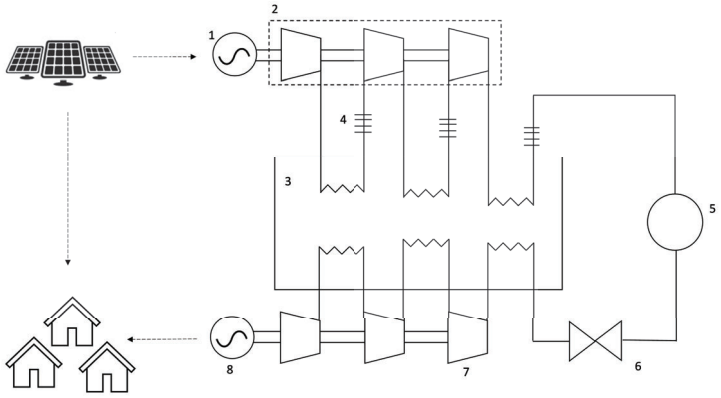

Figure 1: : Scheme of the CAES plant: (1) electric motor, (2) compressor, (3) thermal storage, (4)heatsinks, (5)high-pressure vessels, (6) regulation valve, (7) expander, (8) generator.

3 THERMODYNAMIC MODEL

The system model was developed using the open-source software OpenModelica (Fritzson et al., 2005). This software was selected for its capability to simulate time-evolving systems. The model was developed considering the dynamic and off-design performance of each component to achieve an accurate characterization of the entire plant. The components sub-models are parameterized based on their characteristic dimensions to enable sensitivity analysis based on components size. The considered sub-models represent generic components, albeit of a specific typology (i.e. scroll expanders), modelled using state-of-the art relations, so as to keep the treatment, as well as the procedure's applicability, as general as possible. The main equations are summarized in Table 1. The compression and expansion processes are simulated as adiabatic transformations, characterized by an isentropic efficiency η_{is} that depends on the operating point of the machines. Regarding the outlet compression temperature, a maximum value of 150°C was imposed, to mimic the characteristic limitations of standard machines. The expander, on the other hand, was considered adiabatic. The efficiency curves of compressor and expanders were modelled using the analytical expression proposed by Declaye et al. (2013) reported in Equation (2): ξ is a parameter setting the shape of the efficiency curve; for the expanders, this coefficient was taken from the cited paper, while for the compressor stages, it was derived by fitting in-house retrieved experimental data. Each compression stage is modelled by means of characteristic curves of the isentropic and volumetric efficiency, both expressed as a function of pressure ratio and rotational speed. Figure 2 shows these curves, and the meaning of the coefficients reported in Equation (2), (3), (4) is graphically explained in Figure 2.b. During the simulation of the charging phase, the model starting from the pressure inside the air storage iteratively query the look-up tables, containing the information of characteristic curves, to determine the operating point of each stage. In this way, a value of pressure ratio for each stage and a common rotating speed is calculated like those that make the compressor dispose of the instantly available power without exceeding the maximum allowable velocity. An analogous approach is used for the expander, so that it provides the required power, or the maximum that it can provided according to

https://doi.org/10.52202/077185-0003

its dimension. The heat exchangers are modelled using the "ε-NTU" approach, which is based on the calculation of the heat exchanger effectiveness ε as a function of the number of transfer units, NTU, the heat capacity rate ratio and the flow arrangement in the heat exchanger; this method is widely accepted and used in the literature (Grazzini and Milazzo, 2011). As for the oil and air reservoirs, energy balances were imposed, taking into account the dissipation to the external environment. The temperature inside the tanks is considered uniform throughout the volume. For sake of brevity the equations used to model the expander are not reported in Table 1 since the same approach of the compressor was used.

Table 1: Main equations describing the behavior of CAES components

Component	Equations	
Compressor	$w_{s,i} = \eta_{is,i} \cdot \frac{\gamma}{\gamma-1} \cdot R \cdot T_{c,in,i} \cdot \left(\beta_{c,i}^{\frac{\gamma}{\gamma-1}} - 1\right)$	(1)
	$\eta_{is} = \sin(\xi \cdot \arctan(B \cdot (\beta - \beta_0) - E \cdot (B \cdot (\beta - \beta_0) - \arctan(B \cdot (\beta - \beta_0)))))$	(2)
	$B = \frac{\delta}{\xi \cdot \eta_{max}}$	(3)
	$E = \frac{B \cdot (\beta - \beta_0 - \tan(\frac{\pi}{2\xi}))}{B \cdot (\beta_{max} - \beta_0 - \arctan(B \cdot (\beta_{max} - \beta_0)}$	(4)
Heat exchanger	$h_{h,in} - h_{h,out} = \varepsilon \cdot (h_{h,in} - h_{h,T_c})$	(5)
	$\varepsilon = 1 - e^{NTU}$	(6)
	$NTU = \frac{UA}{c_p \cdot \dot{m}}$	(7)
Air reservoir	$\frac{dU}{dt} = \dot{m_{in}} \cdot h_{in} - \dot{m_{out}} \cdot h_{out} + \dot{Q_{amb}}$	(8)
TES	$T = T_0 + \frac{Q_{hex} + Q_{amb}}{M \cdot c_p}$	(9)

The temporal evolution of the system is driven by the trend of power output from the photovoltaic plant and the power demand from the user. The model simulates the variation of irradiance over time through the OpenModelica library "PhotoVoltaics" (Brkic et al., 2019) which analytically calculates irradiance based on location, data, hour and some date regarding the PV modules (e.g. angle of inclination with respect to the horizontal plane). Figure 3 shows the daily irradiance profile for the selected locality (Florence) for a certain day of January and July. From the irradiance data, the available power is derived by considering the installed peak power and the efficiency of the photovoltaic system ($P_{PV} = \eta_{PV} \cdot I \cdot kW_p$). As for the required power, a typical domestic load profile is considered, with a peak of approximately 11 kW to simulate multiple users, as shown in Figure 4. This profile is cyclically repeated for each day of the year, without considering seasonal variations in load but considering an average load (Joshi, 2017). The compressor's absorbed power and the expanders' generated power are adjusted to align with the load profile, determined by the difference between the PV output and user load curves, by adjusting their rotational speed within the permissible range. However, the presence of limitations on rotational speed and the maximum allowable pressure inside the pressure vessel constrains the ability to store the entire amount of the available energy produced by the PV panels. Two performance indicators were used to assess system's performance: Round-Trip Efficiency (RTE), defined as the ratio of energy produced during the expansion phase to that absorbed by the compressor over a reference period of one year (Eq. (10)), and the Energy Coverage Percentage (ECP), which is defined as the ratio between the total released energy by CAES and the total energy shortage during the same period (Eq. (11)).

$$RTE = \frac{E_{out}}{E_{in}} \tag{10}$$

$$ECP = \frac{E_{out}}{E_{shortage}} \tag{11}$$

https://doi.org/10.52202/077185-0003

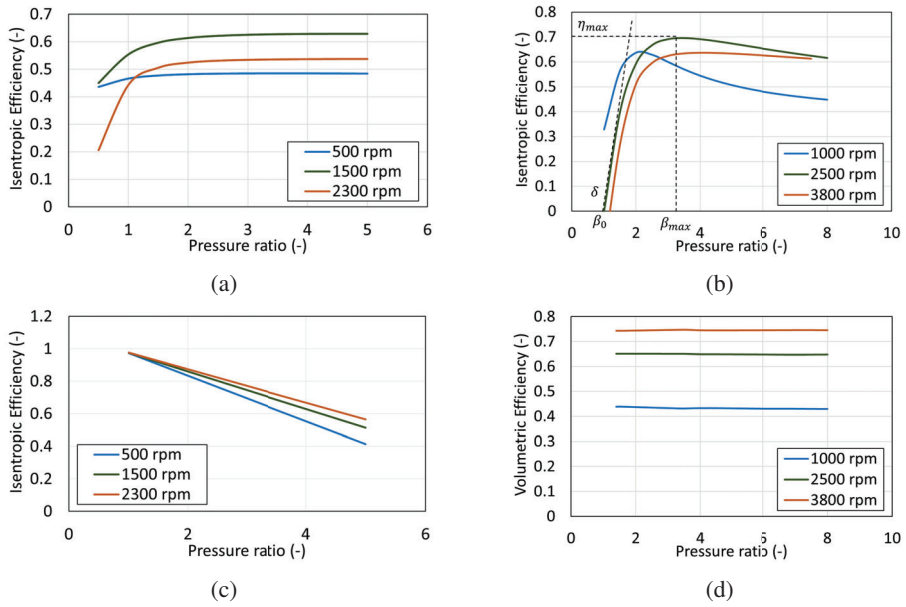

Figure 2: Machines efficiency curves as function of pressure ratio: (a) compressor η_{is}, (b) expander η_{is}, (c) compressor η_{vol}, (d) expander η_{vol}

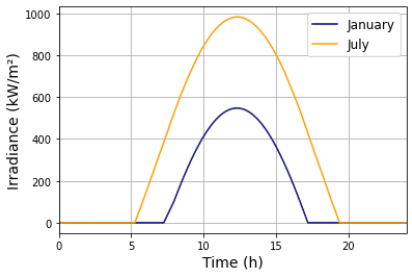

Figure 3: Daily solar irradiance in Florence

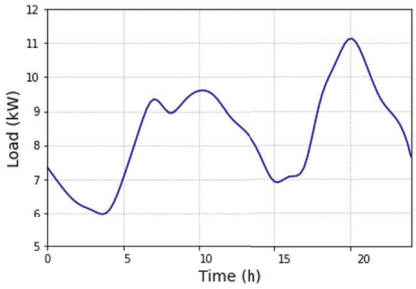

Figure 4: User load profile

4 NUMERICAL METHOD

4.1 Sensitivity analysis

Both the sensitivity analysis and the optimization process were performed by coupling OpenModelica with Dakota, an open-source toolkit that provides an interface between simulation codes and iterative analysis methods (Adams et al., 2020). Dakota's execution is configured through an input file that defines the analysis type and specifies the file names linked to the user's simulation code. While in operation, Dakota automatically executes the user's simulation code by creating a separate external process. The sensitivity analysis aims to evaluate which parameters of the system most significantly impact its performance (RTE and ECP), to evaluate the possibility of excluding some parameters from the optimization process reducing its computational cost. The independent parameters studied in the sensitivity analysis are summarized in Table 2 together with their considered range of variation. The displacements shown in the table refer to the first compression/expansion stage; the volumetric ratio between the various stages is kept constant during the sensitivity analysis and it is based on preliminary evaluation. It has to be pointed out that at least one parameter for each component has been considered, mainly characterizing its size. Other

https://doi.org/10.52202/077185-0003

parameters characterizing the CAES thermodynamic cycle (i.e. max TES temperature, max compressor outlet temperature, . . .) have not been considered, as they are detailed by each component technology level. For this reasons, the maximum compressor temperature and expander inlet pressure have been set to 150°C and 45 bar respectively, as characteristic values for the considered typology of components; for the same reasons the maximum value of the machines efficiency curves have been set as shown in Figure 2. The sensitivity analysis was performed by using the method developed by Morris (1991) with the correction proposed by Campolongo et al. (2007). This method allows to rank the parameters influence on the output, and it was selected since it allows to deal with non-monotonic relationship and to consider interaction between variables differently from simpler approach (e.g. method Spearman and Pearson correlation coefficient). At the same time, it guarantees a low computational cost (i.e. number of simulated points) if compared with others global sensitivity methods based on variance decomposition, such as Sobol index, at a slightly reduced accuracy (Iooss and Lemaître, 2015). As the goal of this stage is to achieve a quick qualitative comparison between the impact of different parameters, the method was considered well suited for it. This method involves a sampling strategy that allows to compute the elementary effect of each input on the output E_i; the final outputs of the method are the modified mean μ_i^* and variance σ_i of the elementary effect. The mean μ_i^* is a measure of influence of the i-th parameter on the output. The grater it is, the more the i-th input contributes to the dispersion of the output. The variance σ_i is a measure of non-linearity and interaction effects of the inputs: low value suggests a linear relationship between input and output while a large value will indicate non-linear effects, or interaction with at least one other variable. Due to the goals described above and to limit the required time, the thermodynamic model was here simulated for a time range of one month, performing the sensitivity analysis for both a winter month (January) and a summer month (July).

Table 2: Studied independent parameters in sensitivity analysis

Parameter	Symbol	Range
Compressor displacement	C_{cc}	500 ÷ 4000 cm^3
Expander displacement	Ex_{cc}	10 ÷ 60 cm^3
Pressure vessels volume	V	10 ÷ 50 m^3
Thermal oil mass	M	2000 ÷ 6000 kg
Max air pressure inside vessels	P_{max}	40 ÷ 200 bar
PV installed power	kW	30 ÷ 150 kW

4.2 Optimization process

Subsequently to the sensitivity analysis, two optimization processes were carried out to identify the plant configuration that maximizes the RTE and the ECP separately. The design parameters that are varied during the optimization process are the same as those examined in the sensitivity analysis, except for those identified as negligible in the sensitivity analysis results. The optimization algorithm used to minimize the objective function (F_{obj}) is based on the Efficient Global Optimization (EGO) methodology. This method was firstly proposed by Jones et al. (1998) to facilitate the minimization of expensive implicit response functions by using a surrogate model of the real one; this method allows to reduce the number of iterations to be carried out compared to other optimization algorithms (A. T. Nguyen et al., 2014). The optimization process is depicted in Figure 5 and here briefly described:

1. Firstly, a set of sample points is generated in the design space using the Optimal Latin Hypercube Sampling (OLHS) providing a good representation of the design space (Park, 1994); the number of initial points is chosen by the algorithm based on the number of variables. For these points the object function is evaluated through the thermodynamic model creating a starting database.

https://doi.org/10.52202/077185-0003

2. The data available in the database are used to build a Gaussian process (GP) approximation for F_{obj}, so it can be approximated by an analytical formulation. (Schulz et al., 2018)
3. The EGO process looks for the point in the design space that maximize an Expected Improvement (EI) function, defined as the expectation that each configuration will provide a better solution than the current best, based on both the expected values and variances computed by the GP model (i.e. points with parameters values that are "far" from the investigated ones will bear a higher uncertainty, thus potentially present a high EI even if the predicted F_{obj} is lower than the current minimum).
4. Modelica analysis is then performed for the parameters that maximize the EI to evaluate the real value of F_{obj} in this point.
5. Finally, a convergence check is performed at each iteration, if the criterion is met the loop ends, otherwise the optimization loop is continued, and the database is updated with the value computed in the previous step, to create an updated surrogate. The convergence criteria here used is based on the value of EI being lower than 0.001 for two consecutive iteration.

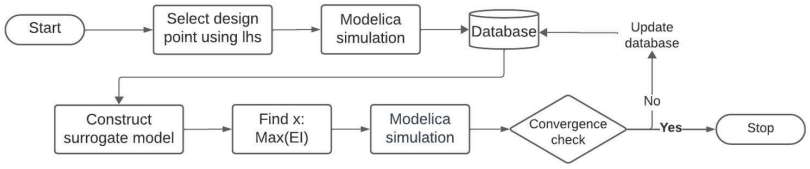

Figure 5: Optimization process workflow

5 RESULTS

5.1 Results of the sensitivity analysis

The sensitivity analysis results are depicted in Figure 6 using the Morris plot in which the values obtained for each output are represented in a $\mu^* - \sigma$ plane. The plots show that, for both outputs the parameters with the greatest influence are the installed power and the compressor displacement, while the least influential parameter for both outputs, in both seasons, is the mass of the thermal oil. Other parameters exhibit a different behaviour between seasons. For instance, the influence of the expander displacement is the second least influential parameter concerning the round-trip efficiency in the summer months, but it is much more influential in the winter months. This is due to the different average inlet pressure to the expander: in the summer, when a generally high inlet pressure is guaranteed by a higher PV power excess, it manages to consistently operate nearly its design point. In contrast, during the winter months, when the inlet pressure is generally lower, only low displacement values result in high enough rotational speeds to guarantee a good efficiency; therefore its influence is considerable. In terms of energy coverage, seasonal disparities are more pronounced. In winter, the most relevant parameter is the installed power, since it is crucial to install a high power in order to accumulate enough energy to compensate for energy shortages. In summer, on the other hand, the volume of the air tanks is more relevant, because when there is plenty of energy available from PV, it is important to choose it correctly to ensure the correct capacity of the system. Since μ^* and σ have the same order of magnitude for all parameters it can be deduced that there are relevant interaction effects among the variables. This confirms how crucial it is to properly size the system, considering the mutual relationships between components. Comparing the values that μ^* and σ assume for the two outputs a significant average difference can be noticed. This can be explained by the fact that, within the explored range, the energy coverage exhibits a much higher variation ($0.3 \div 0.9$) compared to the one of round-trip efficiency ($0.15 \div 0.27$). The RTE, in fact, depends heavily on the efficiency of the machines, which is not a parameter that can be chosen during the plant design but is rather due to technological limits of the machines. Based on the reported results, it was decided to

https://doi.org/10.52202/077185-0003

exclude the oil mass from the parameters considered in the optimization process. Its effect is not entirely negligible, but constantly lower than the one of the other parameters for every considered output and month, therefore it can be excluded to reduce the complexity and duration of the process, assigning to the mass the lowest value within the study range to minimize the cost without significantly affecting the performance.

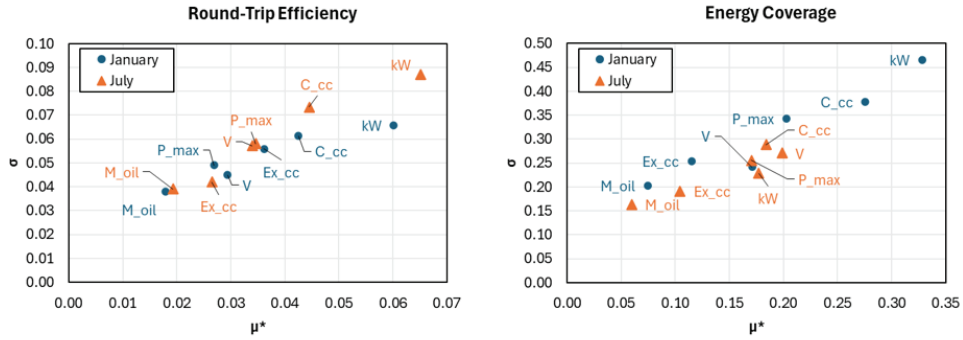

(a) (b)

Figure 6: Sensitivity analysis results in Morris plot: (a) RTE (b) ECP

5.2 Results of the optimization process

This section presents the results of the EGO optimization, while the potential utilization of the surrogate model developed during the optimization phase is discussed in the subsequent section. The parameter ensuring the best values for the objective functions are shown in Table 3. It can be seen that a maximum ECP of 93% can be achieved; higher values could not be achieved, even with increased PV power, since a small amount of energy, required at very low power, can not be provided, as the expander would need to operate at a too low rotational speed, for its allowed limits. The optimized RTE value reaches 0.28; although not particularly high, it is a quite common value when it comes to simple CAES systems and higher values are generally reached only at the expense of non-conventional components (i.e. isothermal operating compressor/expander, constant pressure storages) or complicated layouts (i.e. higher number of compressor/expander stages) (T. Kim et al., 2022; Y. M. Kim et al., 2011). A few considerations can also be made regarding the optimized parameters values. Obviously, a high installed PV power is necessary to reach a high energy coverage, as well as a high maximum storage pressure, so to store the maximum amount of energy. In terms of best RTE, both values significantly drops, so to reduce the amount of energy that is stored at a pressure higher than 45 bar (i.e. maximum allowed inlet pressure at the expander) and therefore the energy loss by lamination. Still, it has to be noted that the optimum P_{max} value is higher than 45bar: storing at slightly higher pressure can be, in fact, beneficial, as a trade-off between limiting the extent of lamination and letting the expander work at high pressure ratio, where the maximum isentropic efficiency is achieved. The optimized storage volume value is the maximum allowable when optimizing energy coverage, as its size is directly linked to the total energy capacity of the storage. Conversely, a lower value is advantageous for optimizing RTE, as it ensures the machine operates at an optimal pressure ratio for an extended duration throughout the year. Additional considerations regarding compressor and expander size will be made in the following analyses. To check the convergence of the optimization process, the evolution of the expected improvement is plotted on Figure 7, for sake of brevity henceforth results are analysed only for the RTE optimization process, similar results are obtained for energy coverage. Figure 7 shows that EI starts from a value above 0.035 and it decreases rapidly to reach a value below the convergence limit in 41 iterations. The decrease of the EI is associated not only with a reduction in the probability of finding an improved configuration, but also with a more correct

https://doi.org/10.52202/077185-0003

prediction of the objective function by the surrogate model. This aspect is illustrated by Figure 8 that shows the comparison between the value predicted by the surrogate model and the value calculated by the thermodynamic model for each iteration. These results show that the optimisation process has achieved adequate convergence and provides a reliable representation of the actual model.

Table 3: Optimal configurations predicted by EGO

$C_{cc}(cm^3)$	$Ex_{cc}(cm^3)$	$V(m^3)$	$PV(kW)$	$P_{max}(bar)$	$RTE_{max}(-)$	$ECP_{max}(-)$
2833	21	36	88	54	0.28	-
3063	20	50	150	170	-	0.93

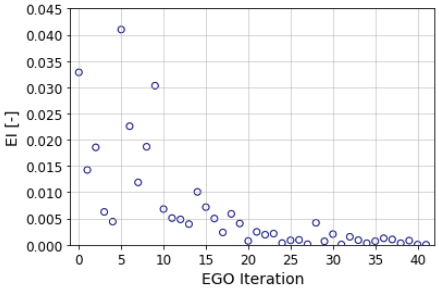

Figure 7: Evolution of expected improvement

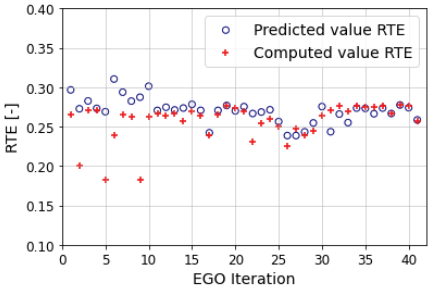

Figure 8: Comparison of predicted and exact value of RTE

5.3 Use of the surrogate model

An useful characteristics of the adopted procedure is the fact that the surrogate model obtained at the end of the optimisation can be utilized to preliminary evaluate, without relying on the thermodynamic model (i.e. with significantly increased speed), the performance of the system in areas of the design space different from the optimized configurations. To provide examples of possible applications, the two Kriging models were used in combination to identify the Pareto frontier in the RTE-ECP space, as shown in Figure 9. The curve allows to estimate the maximum achievable RTE of the system, once a certain minimum ECP constraint is considered. For some configurations, the corresponding installed kW value has been reported. The trend shows that moving from left to right along the curve, as the installed kW increases, the energy coverage increases at the expense of a slight reduction in efficiency. In this region, the increase in kW corresponds to an increase in volume, resulting in a slight change in operating pressure levels. Beyond a certain limit, this is no more possible and a significant drop in the RTE is achieved, to reach the maximum ECP values. Additionally, the Pareto curve can be used to identify the configuration with the best trade-off between the two objective functions (red circle), defined as the one that minimizes the distance from the ideal point characterized by the maximum value of both parameters. This point represents the best system configuration in the absence of other assumptions that would assign a decision weight to the two parameters. Table 4 shows the parameter values for this configuration and the performance computed by both the surrogate models and the thermodynamic model showing that the surrogate predicts the performance with an error lower than 1%. Another application of the surrogate model is depicted in Figure 10. In this case it is used to evaluate the variation of the performance parameters, once variation in compressor/expander size is enforced. To provide an effective representation, the values of the other parameters have been fixed to the optimized values of Table 3; therefore, the results show the sensitivity to machines choice for configurations aimed at maximizing either the ECP (i.e. high solar power and storage pressure) or the RTE (i.e. limited solar power and storage

https://doi.org/10.52202/077185-0003

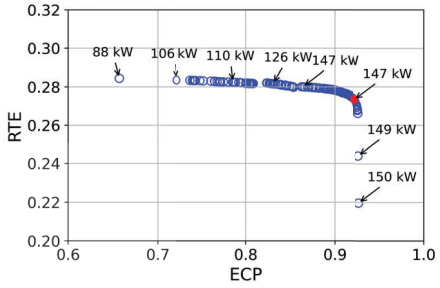

Figure 9: ECP-RTE Pareto front of the CAES system derived from the surrogate model

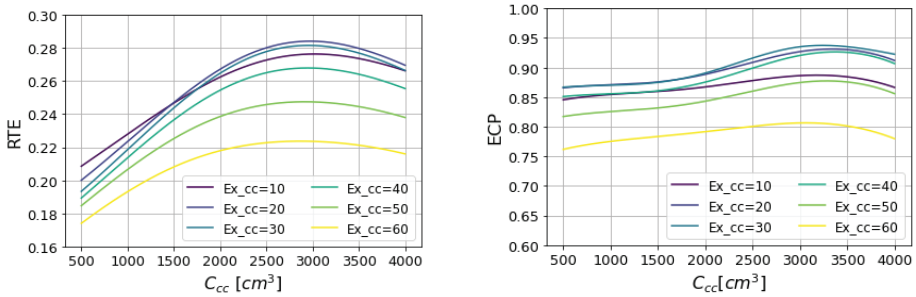

(a) (b)

Figure 10: Map of the system performance for varying machines size - RTE (a) and ECP (b)

pressure). Concerning the RTE, the depicted curves allow to identify an area close to the maximum in which there is minimum efficiency variation ($20cm^3 < Ex_{cc} < 30cm^3; 2500cm^3 < C_{cc} < 3500cm^3$), this consideration would not have been derived from the EGO results without exploring the design space more thoroughly. It is dutiful to note that the curves show how the surrogate predicts a maximum for values slightly different from those obtained at the end of the optimisation process, however, the deviation of the RTE value is negligible. Generally, the trend shows that a reduction in the displacement of the expander allows an improvement in efficiency since by reducing its size the expander will operate at a high rotation speed that is associated to a higher efficiency, especially due to the reduction of leakage effects, that are of main relevance for this type of expander. The displacement of the compressor is optimal around 3000 cm^3 as a smaller displacement would limit the stored energy (due to maximum rotational speed limitations) and therefore the pressure that can be reached inside the pressure vessels, causing the compressor to operate at sub-optimal pressure ratio. Concerning energy coverage, reducing the displacements compromises the performance as it won't be possible to accumulate all the necessary energy, while increasing them too much would result in working at low rotational speeds associated with sub-optimal efficiency. The surrogate model thus proves to be a suitable tool for quick preliminary evaluations, beneficial for industrial applications where, following optimisation, one wishes to evaluate the sensitivity of the system performance to the parameters choice, e.g. to estimate the performance that could be achieved by using components available on the market.

Table 4: Optimal trade-off configuration predicted on Pareto front

C_{cc}	Ex_{cc}	V	PV	P_{max}	RTE_{surr}	ECP_{surr}	RTE_{tm}	ECP_{tm}
$3361cm^3$	$15cm^3$	$37m^3$	147kW	83bar	92.2%	27.3%	91.6%	27.3%

https://doi.org/10.52202/077185-0003

6 CONCLUSIONS

This article presents an approach to modelling and optimising a micro-scale CAES system. A thermodynamic model was developed using the open-source software OpenModelica to accurately represent its off-design performance. The model was used to simulate the operation of the system in an off-grid configuration, connected to a PV source and domestic users, for a full year. The model was coupled with an external tool to perform both sensitivity analysis and optimisation. The sensitivity analysis highlighted the significant impact of parameters such as compressor displacement and installed power on system performance, while also revealing seasonal variations in parameter influence. It also identified thermal oil mass as the less influential parameter, leading to its exclusion from the subsequent optimisation process. The optimisation process, based on the EGO methodology, efficiently identifies optimal configurations that maximise round-trip efficiency (RTE) or energy coverage (ECP) by using a surrogate that is iteratively updated with the output from the thermodynamic model. The optimisation process converges to optimal solutions within a reasonable computational time and ensures an accurate representation of the thermodynamic model. In addition, the study discusses the potential post-optimisation use of the surrogate model, allowing rapid evaluation of system performance across the design space. The developed procedure thus showed good application potential and could be used in further work to study the influence of design parameters on other objective functions, e.g. the levelized cost of electricity (LCOE).

NOMENCLATURE

Latin Symbols

E	Energy (J)
cc	displacement (m^3)
cp	Constant pressure heat capacity (J/kgK)
h	Enthalpy (J)
I	Irradiance (kW/m2)
kW_p	Installed photovoltaic peak power (kW)
$\dot{m}$	Mass flow rate (kg/s)
n	Rotational speed (rpm)
R	Specific gas constant (J/kgK)
T	Temperature (°C)
U	Internal energy (J)
UA	Global heat transfer coefficient (W/K)
w	Specific work (J/kg)

Greek Symbols

β	Pressure ratio (-)
$\beta_{\max}$	Optimal pressure ratio (-)
β_0	Pressure ratio for which isentropic efficiency is zero (-)
η_{PV}	Photovoltaic system efficiency (-)
γ	Heat capacity ratio (-)
δ	Isentropic efficiency slope where isentropic efficiency is zero (-)
ξ	Shape factor for efficiency curve (-)

Superscripts and Subscripts

0	Initial condition
amb	Ambient
c	Cold side
h	Hot side
i	i-stage
in	Inlet
is	Isentropic
out	Outlet
surr	Predicted by the surrogate
tm	Computed by the thermodynamic model
vol	Volumetric

REFERENCES

Adams, B. M. et al. (2020). *Dakota, a multilevel parallel object-oriented framework for design optimization, parameter estimation, uncertainty quantification, and sensitivity analysis: version 6.13 user's manual*. Tech. rep.

Bazdar, E. et al. (Oct. 2022). *Compressed air energy storage in integrated energy systems: A review*.

Brkic, J. et al. (2019). "41 Open Source PhotoVoltaics Library for Systemic Investigations". In.

Campolongo, F., J. Cariboni, and A. Saltelli (Oct. 2007). "An effective screening design for sensitivity analysis of large models". In: *Environmental Modelling and Software* 22 (10), pp. 1509–1518. ISSN: 13648152.

Cheayb, M. et al. (Jan. 2022). "A techno-economic analysis of small-scale trigenerative compressed air energy storage system". In: *Energy* 239. ISSN: 03605442.

https://doi.org/10.52202/077185-0003

Congedo, P. M. et al. (Sept. 2022). "Optimization of Micro-CAES and TES Systems for Trigeneration". In: *Energies* 15 (17).
Declaye, S. et al. (June 2013). "Experimental study on an open-drive scroll expander integrated into an ORC (Organic Rankine Cycle) system with R245fa as working fluid". In: *Energy* 55, pp. 173–183. ISSN: 03605442.
Dehghani-Sanij, A. et al. (2019). "Study of energy storage systems and environmental challenges of batteries". In: *Renewable and Sustainable Energy Reviews* 104, pp. 192–208.
Fritzson, P. et al. (2005). "The openmodelica modeling, simulation, and software development environment". In: *Simulation News Europe* 44, pp. 8–16.
Garvey, S. D. and A. Pimm (Apr. 2016). "Compressed Air Energy Storage". In: Elsevier Inc., pp. 87–111.
Grazzini, G. and A. Milazzo (2011). "A thermodynamic analysis of multistage adiabatic CAES". In: *Proceedings of the IEEE* 100.2, pp. 461–472.
Guo, C. et al. (Jan. 2019). "Comprehensive exergy analysis of the dynamic process of compressed air energy storage system with low-temperature thermal energy storage". In: *Applied Thermal Engineering* 147, pp. 684–693.
He, W. (May 2018). *Optimal selection of air expansion machine in Compressed Air Energy Storage: A review*.
Heidari, M., D. Parra, and M. K. Patel (Mar. 2021). "Physical design, techno-economic analysis and optimization of distributed compressed air energy storage for renewable energy integration". In: *Journal of Energy Storage* 35.
Iooss, B. and P. Lemaître (2015). "A review on global sensitivity analysis methods". In: *Operations Research/ Computer Science Interfaces Series* 59, pp. 101–122. ISSN: 1387666X.
Jannelli, E. et al. (Dec. 2014). "A small-scale CAES (compressed air energy storage) system for stand-alone renewable energy power plant for a radio base station: A sizing-design methodology". In: *Energy* 78, pp. 313–322.
Jones, D. R., M. Schonlau, and W. J. Welch (1998). *Efficient Global Optimization of Expensive Black-Box Functions*.
Joshi, K. (2017). *Sustainable Energy Systems with Photovoltaic Generation and Energy Storage Solutions for Rural Communities in India and Canada*. URL: https://www.researchgate.net/publication/316998445.
Karapekmez, A., I. Dincer, and N. Javani (Dec. 2020). "Development of a new integrated energy system with compressed air and heat storage options". In: *Journal of Energy Storage* 32. ISSN: 2352152X.
Kim, T. et al. (Dec. 2022). *A review on nearly isothermal compression technology*.
Kim, Y. M., D. G. Shin, and D. Favrat (2011). "Operating characteristics of constant-pressure compressed air energy storage (CAES) system combined with pumped hydro storage based on energy and exergy analysis". In: *Energy* 36 (10), pp. 6220–6233. ISSN: 03605442.
King, M. et al. (Apr. 2021). "Overview of current compressed air energy storage projects and analysis of the potential underground storage capacity in India and UK". In: *Renewable and Sustainable Energy Reviews* 139.
Mohler, D. and D. Sowder (2017). "Energy Storage and the Need for Flexibility on the Grid". In: *Renewable energy integration*. Elsevier, pp. 309–316.
Morris, M. D. (1991). *American Society for Quality Factorial Sampling Plans for Preliminary Computational Experiments*.
Mucci, S. et al. (Sept. 2021). "Small-scale adiabatic compressed air energy storage: Control strategy analysis via dynamic modelling". In: *Energy Conversion and Management* 243. ISSN: 01968904.
Nguyen, A. T., S. Reiter, and P. Rigo (2014). *A review on simulation-based optimization methods applied to building performance analysis*.
Nguyen, T.-T. et al. (2017). "A review on technology maturity of small scale energy storage technologies". In: *Renewable Energy and Environmental Sustainability* 2, p. 36.
Park, J.-S. (1994). *Optimal Latin-hypercube designs for computer experiments*.*
Schulz, E., M. Speekenbrink, and A. Krause (Aug. 2018). "A tutorial on Gaussian process regression: Modelling, exploring, and exploiting functions". In: *Journal of Mathematical Psychology* 85, pp. 1–16. ISSN: 10960880.
Tumminello, D. et al. (Dec. 2023). "Numerical modeling and exergetic analysis of efficiency improving solutions for a micro-CAES system". In: *Journal of Physics: Conference Series* 2648 (1), p. 012045. ISSN: 1742-6588.
Yao, E. et al. (June 2016). "Thermo-economic optimization of a combined cooling, heating and power system based on small-scale compressed air energy storage". In: *Energy Conversion and Management* 118, pp. 377–386.
Zhou, Q. et al. (Dec. 2019). *A review of thermal energy storage in compressed air energy storage system*.

ACKNOWLEDGEMENT

The authors wish to gratefully acknowledge GFM spa for the possibility to publish the results and for partially funding the research.

https://doi.org/10.52202/077185-0003